Dynamic postbuckling behaviour of eccentrically laminated axially compressed circular cylinders

Luc Wullschleger* — **Hans-Reinhard Meyer-Piening**

ETH Zürich, Institut für Mechanische Systeme IMES/ST
Leonhardstrasse 27
CH-8092 Zürich

luc@lucwulli.ch
Hans-Reinhard@Meyer-Piening.ch

ABSTRACT. *The buckling of axially compressed cylindrical shells is a dynamic phenomenon characterized by rapid movements of the shell in radial direction. This transition from the pre-buckling state to a post-buckling state was calculated by FE analyses for two substantially different cylindrical CFRP shells. The buckling loads of these shells differ by almost a factor of two and the post-buckling states of equilibrium only by a minor amount. A sequence of pictures of the intermediate deflection pattern has been assembled, showing the complex transition from the unbuckled state into the stable condition after buckling. It can be seen that both specimens show considerable difference in their dynamic behaviour. Furthermore it could be verified that nonlinear static stability investigations and dynamic analyses yield very similar results for the buckling loads.*

RÉSUMÉ. *Le flambage dynamique de cylindres en compression axiale se caractérise par des mouvements rapides dans la direction axiale. Le papier présente la simulation éléments finis de la transition entre les états pré et post flambés de deux cylindres composites significativement différents. Une des charges critiques est environ deux fois supérieure à l'autre alors que les états finaux post flambés sont très voisins. Une suite de figures montre une très grande différence des formes pendant la transition dynamique. On peut également vérifier que le prévision des charges critiques en statique ou en dynamique non linéaire sont très voisines.*

KEYWORDS: *buckling, postbuckling, shells, composites, dynamic analysis*

MOTS-CLÉS : *flambage, statique dynamique, post flambage, composites*

1. Introduction

Thin-walled circular cylinders have a tendency to respond with undesired dynamic amplitudes when loaded by compressive membrane stresses beyond instability limits. Severe dynamic movements of the shell in radial direction characterize the transition from the pre-buckling state to a post-buckling state of equilibrium. During such displacements the initial buckling pattern transforms rapidly into a stable post-buckling pattern.

When DLR Braunschweig (former DFVLR) was performing experiments in the late sixties with circular cylinders made of Hostaphan (Mylar) the experimenters became interested in the dynamic behaviour of the shell wall during buckling. With high-speed movies [ESS] it was visible that, in the case of elastic shell material and axial loading, the initial buckling pattern was not similar to the post-buckling pattern that can be detected after the shell came to a rest. This fact brought investigations to a certain halt in which the experimental post-buckling patterns were studied with reference to their criticality regarding the onset of buckling.

Static FE analysis methods in general result in a buckling load and a respective buckling pattern, but they give neither information about the post-buckling load nor the post-buckling patterns that can be observed during tests. In turn, the patterns resulting from classic analyses, in the majority of cases, cannot be observed without technical aid due to the high velocity of shape changes within the transition. With high-speed movies it is possible to visualize the initial buckling patterns, but such investigations require complex optical equipment. Based on the high-speed movies of the Mylar cylinder, dynamic transient FE analyses were performed which show reasonable agreement of the behaviour of such cylinders. The usability of this numerical method for the buckling analyses of shells was already demonstrated in [KRO 86] and [BIS 00]. The dynamic transient analysis of the Mylar cylinder was performed basically to calibrate the dynamic calculations, as for other cylinders no high-speed movie is available. These calculations finally also provided the basis for reliable static and dynamic transient analyses of cylinders having parametric dimple imperfections as introduced in [WUL 02], for which only these numerical methods could be used.

As orthotropic properties with non-zero coupling terms may affect the buckling behaviour of cylindrical shells, the dynamic analysis was applied to such shells and the results are reported in the following.

2. Dynamic transient FE analysis of an isotropic cylinder

In the meantime, FE software became available to reproduce the dynamic buckling process. If mass densities are specified for the shell elements then a dynamic response FE analysis can be conducted in which each successive axial-shortening increment is considered to be a dynamic step of axial edge displacement applied to the deformed structure throughout the nonlinear pre-buckling analysis. Since controlling cylinder edge load leads to disastrous deformations at buckling the post-buckling in-

vestigations were in general limited to axial shortening as the loading parameter. As the system remains always in a dynamic equilibrium, this analysis method allows the iteration throughout the sudden change of reaction loads into the post-buckling states of equilibrium. At buckling condition, the buckling pattern develops and the shell is accelerated to exhibit dynamic deflections into the post-buckling state. The maximum reaction force, i.e. the buckling load, is slightly higher than in static analyses due to inertia loads.

By assigning significant damping to the elastic system, the motions can be controlled to a certain extent. In case of an ideal cylinder shape the drop of the reaction force is almost vertical. Thus, the load increments, i.e. the time steps respectively, have to be sufficiently small. Applying damping may help to increase the step size in this critical range. For transient dynamic FE analysis structural damping is in general introduced as a linear combination of mass and/or stiffness matrices (Rayleigh damping). The higher the damping parameter the longer the time steps may be chosen at a pre-selected constant compression velocity. If the number of steps is too restricted real test loading durations may not be adequately modelled (no "crash analysis"). Further, realistic damping parameters are difficult to define and are probably too low to guarantee dynamic equilibrium during the mentioned critical stage with a given (higher) compression velocity and (smaller) number of time steps. Therefore a compromise between these parameters has to be found for each analysis case.

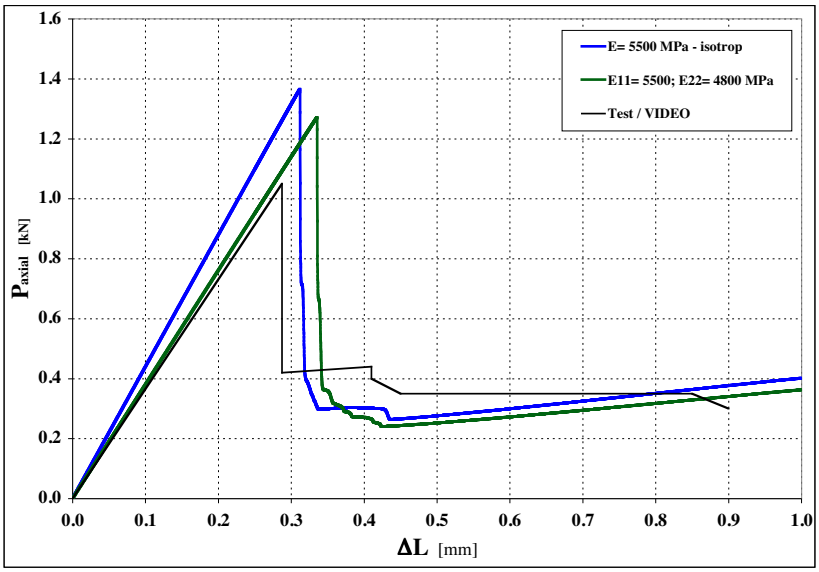

Figure 1. *Results of transient dynamic FE calculations for a Hostaphan cylinder with isotropic material and for somewhat othotropic properties, compared with a corresponding curve found in a high-speed movie. The damping matrix was estimated to be 50 000 times the mass matrix*

To gain the experience needed for calculations of other cylinders without high-speed movies available FE analyses of the Hostaphan cylinder was performed. The investigated isotropic cylinder, matching the above mentioned high-speed movies, had a diameter of 200 mm, a length of 200 mm, a wall thickness of 0.254 mm and a Young's modulus of about 5500 MPa (in axial direction). The assigned mass density was 1400 kg/m^3 and the damping matrix was introduced as about 50 000 times the mass matrix (pure inertia damping). The selected smallest time step for an axial displacement increment was 0.001 s. The implemented FE program was MSC.MARC 2000 and 10 800 thick isoparametric rectangular shell elements (no. 75, bi-linear) had been used. For numerical time integration an implicit method was selected (Single-

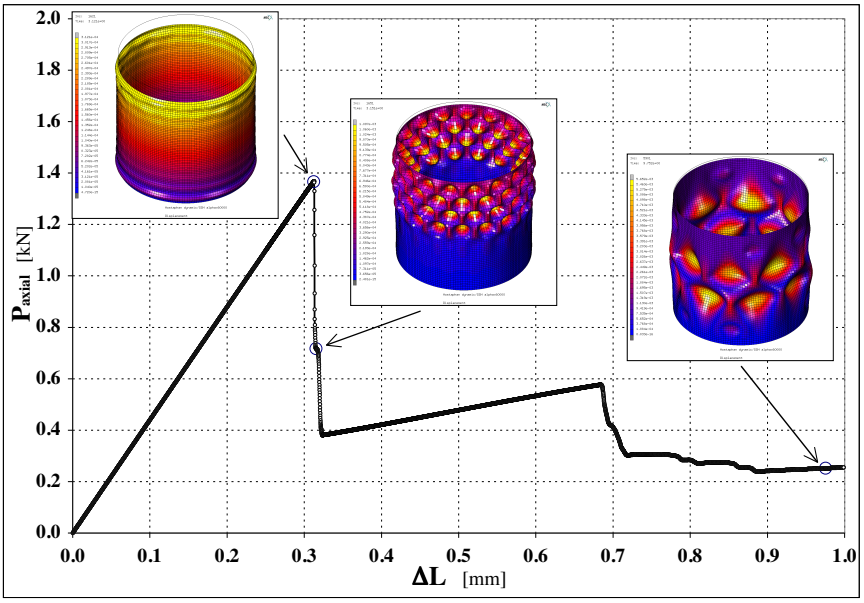

Figure 2. *Results of a dynamic FE analysis of the isotropic cylinder, but with higher damping introduced: damping matrix 60 000 × mass matrix. The deformations plotted in the included pictures are automatically scaled up referring the particular largest value*

step Houbolt, [CHU 94]). The results of such calculations are given in Fig. 1 for ideal geometry and with stiffness properties as indicated in the figure. These curves are compared with the curve reproduced from the movie taken during the test. It was possible to arrange the output of successive deformation states as to create a simulated movie and the results proved to be rather similar to what had been discovered in the high-speed movies. The instability started from a zone near the edge(s) which are laterally constraint by rigid endplates. The first buckle then multiplies, travels throughout the shell, increases in size and settles towards the center of the shell in two staggered rows of buckles. This pattern was then recorded as first stable post-buckling pattern, see Fig. 2.

The obtained results were considered satisfying and, thus, stimulated further investigations with this software in order to study unusual or unexpected buckling phenomena.

3. The orthotropic cylinders

In the late nineties, DLR and ETH Zurich, together with EMPA-Dübendorf, had co-operated in a Brite EURAM effort to study the buckling behaviour of laminated cylinders, to be investigated for their use as shell for a new helicopter tail structure (Eurocopter). The summary of these related analyses and tests are published in [MEY 01].

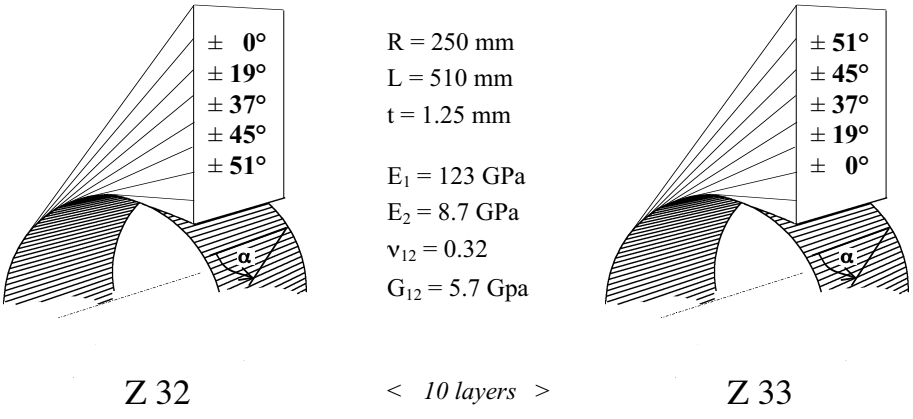

Figure 3. *Cylinder data of specimen Z 32 and Z 33. Note that in the case of specimen Z 33 the axially stiff layers are positioned at the inside. The stacking of specimen Z 32 is just reversed*

Throughout these tests it was discovered that cylinders with identical dimensions, identical membrane and bending stiffness (identical ply directions) but reversed stacking sequence (resulting in merely opposing sign in the coupling stiffness matrix for the shell) experienced a strikingly different buckling behaviour. When the predominantly axially stiff layers were arranged at the outside of the cylinder (specimen Z 32) the shell buckled at nearly half the load value compared to the shell which had the stacking sequence reversed and the more axially oriented fibers positioned at the inside (Z 33). Further information about these specimens is contained in Figure 3.

Immediately prior to buckling the development of an axisymmetric deflection pattern was recorded during the tests by Moiré pictures (Fig. 4) although the postbuckling pattern was non-axisymmetric. This effect was not detectable for specimen Z 33. It became of interest to study the transition by dynamic transient FE analysis.

Figure 4. *Moiré pattern of cylinder Z 32 close to buckling. Horizontal strips represent ring buckles in the pre-buckling state!*

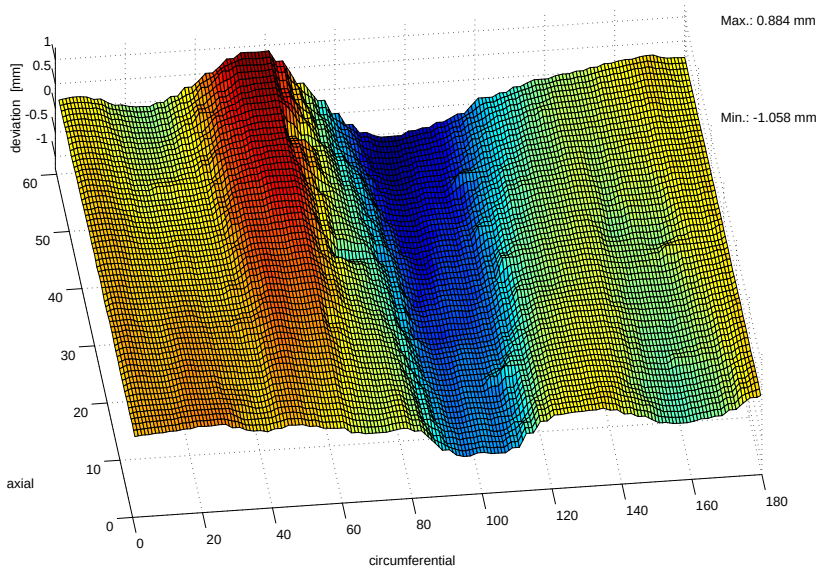

Figure 5. *Imperfections of cylinder Z 33, measured prior to testing at inner surface. Max. deviation from nominal radius (250 mm) is 1.058 mm inwards*

Prior to the test campaign the specimens had been measured in radial direction to allow inclusion of their actual geometric shape in the FE models, ignoring any influence of potential, though unknown, stress disturbances or load variations. In the following, analysis results are reported including the assumption of ideal geometry

and those of the "imperfect" geometry. In case of specimen Z 33, see Fig. 5, a slightly nose-shaped distortion was recorded near one edge – potentially a result of edge bonding and probably connected with an internal –unknown– stress field.

4. Static results for laminated cylinders

Linear buckling analysis is considered to be the standard method for more elaborate investigations on shells under static loading. For FE calculations this procedure consists of the evaluation of an eigenvalue problem resulting in eigenvalues and related normalised mode shapes. This linear analysis method yields a factor to be applied to the considered static state of stress. Singularity investigation of system matrices at buckling is also applied in nonlinear analysis accounting for large displacements and rotations. Nonlinear buckling considers a load-dependent pre-buckling deformation

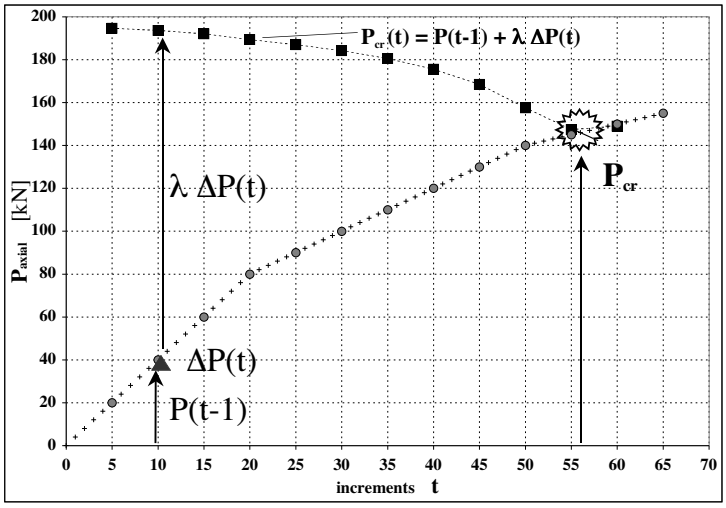

Figure 6. *Scheme of a nonlinear static buckling analysis (example: cylinder Z 33 with measured imperfections)*

during loading up to the structural instability. After a selected number of small load or edge displacement increments a linear eigenvalue investigation may be performed to determine the stability of the investigated pre-buckling state of stress and deformation. At buckling the nonlinear pre-buckling state of stress coincides with the buckling stress (Fig. 6).

In the current work, the static nonlinear buckling analyses were performed using MSC.MARC 2000 with 10 800 of thick shell elements. This procedure yielded little difference to the linear analysis results in the case of ideal geometry but had noticeable influence on the results of cylinders with imperfect geometry. The results of the computations can be found in Table 1. It can be seen that Z 32 has significantly lower

[kN]	*linear* ideal geometry	*linear* imperfections	*nonlinear* ideal geometry	*nonlinear* imperfections	TEST
Z32	105	105	105	103	89
Z33	200	195	199	145	184

Table 1. *FE buckling analysis results*

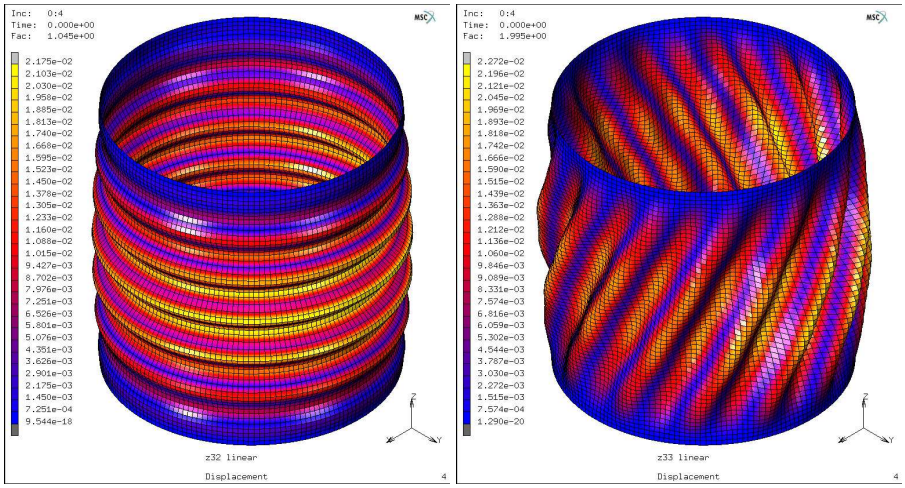

Figure 7. *Linear buckling pattern of cylinders Z 32 (left) and Z 33 (right)*

buckling loads than Z 33. A mechanical explanation can be found in [GEI 02]. In the case of specimen Z 32, the buckling pattern was indeed of axisymmetric shape with 13 half waves in axial direction, matching the Moiré pictures obtained during testing (Fig. 7, left). The “irritating” spiral buckling pattern of cylinder Z 33 could neither be measured nor described by classical analytical solutions (Fig. 7, right).

The influence of the measured imperfection geometry was minor in the case of Z 32 with the low buckling loads. For Z 33, the reduction of the load-carrying capacity was overestimated after the real geometry was accounted for, potentially due to the fact that built-in stresses within the shell are generally ignored.

5. Dynamic results for laminated cylinders

The important differences between static buckling pattern and measured post-buckling pattern was a motivation to investigate the dynamic transition including the post-buckling behaviour. As in the case for the Hostaphan cylinder the dynamic analysis was also conducted with help of MSC.MARC. In this case the assigned mass density was 1600 kg/m^3. The damping matrix was introduced as 25 000 times the

mass matrix. Again, the compression velocity was 0.1 mm/s. Other parameters remained equal to the static analysis.

The result of such analysis for cylinder Z 32 with ideal cylinder geometry is plotted in Fig. 8. The constant reaction force at buckling for about 0.1 mm of compression is special in this case is. The axisymmetric deformation pattern, known from static analysis and tests, is already developed prior to reaching the buckling load. This load is identical to the value achieved by nonlinear static analysis (105 kN). The change to the first post-buckling state starts with non-axisymmetric waves on the top and in the valleys of the middle axisymmetric waves. The post-buckling pattern is clearly different to the pattern achieved by other analyses.

Figure 9 shows the results for the above cylinder with measured imperfections added to the cylinder geometry. The constant reaction force at buckling in the case of ideal geometry (Fig. 8) is replaced by a reduction of the global stiffness close to the buckling load, which is only slightly smaller than the value for the ideal cylinder geometry, but again almost identical to the value produced by a nonlinear static analysis (103 kN). The imperfections are to a certain extent similar to those of specimen Z 33 (Fig. 5). The first picture in Fig. 9 with scaled-up deformations may give a hint of their small modulating effects. The final post-buckling pattern and the corresponding reaction force are identical to the case of ideal geometry. The sector between buckling and this final state is affected by possible dependencies on analysis input parameters (see later).

In Figure 10 the results of a dynamic analysis for cylinder Z 33 with ideal geometry are shown and the improved buckling resistance compared with cylinder Z 32 can be seen. In this case the collapse is significant, manifested by the sharp angle at buckling and the vertical "downfall" of the load vs. axial deflection curve. The buckling load is slightly higher compared with the results in Table 1 (207 kN). The deformation pattern very close and prior to buckling is similar to the mode resulting from a linear buckling analysis (Fig. 7). When compression is increased, this shape is quickly replaced by small buckles starting at one edge. After having filled up the entire surface, the buckles increase and get reduced in number until the state of a first stable post-buckling pattern with two staggered rows of larger buckles is attained.

Applying measured imperfections (Fig. 5), the analytical buckling resistance of cylinder Z 33 is significantly reduced (see Fig. 11). The remaining buckling load is 145 kN, again identical to results achieved by static nonlinear analysis. The small dents in the imperfection surface (Fig. 5) can be well recognised in the first two pictures with scaled-up deformation plots. The fact that with the presented result we underestimated the test result (Table 1) may possibly be explained by the non-consideration of potential pre-stresses. Again, the post-buckling pattern and the corresponding reaction force are identical to the case of ideal geometry.

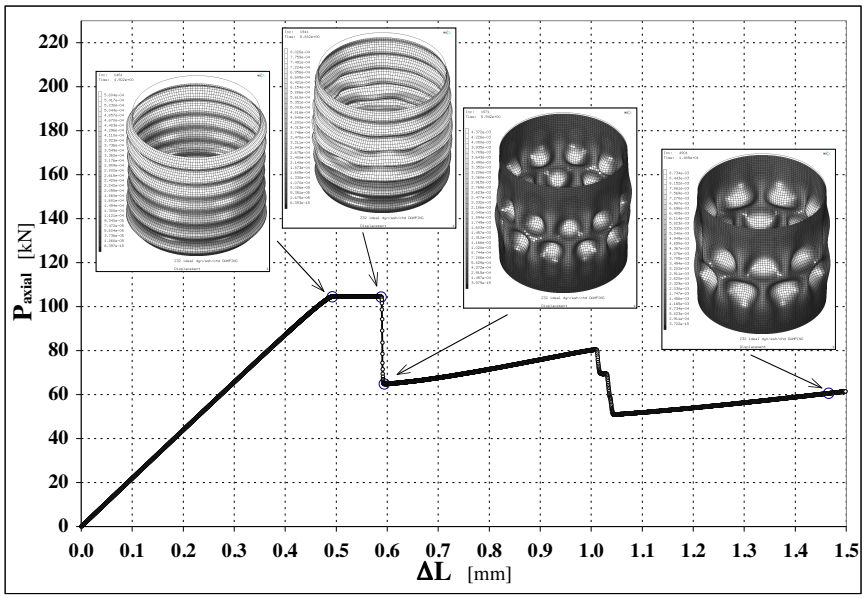

Figure 8. *Dynamic FE analysis results of cylinder Z 32 with ideal geometry. Again, the plotted patterns are automatically scaled*

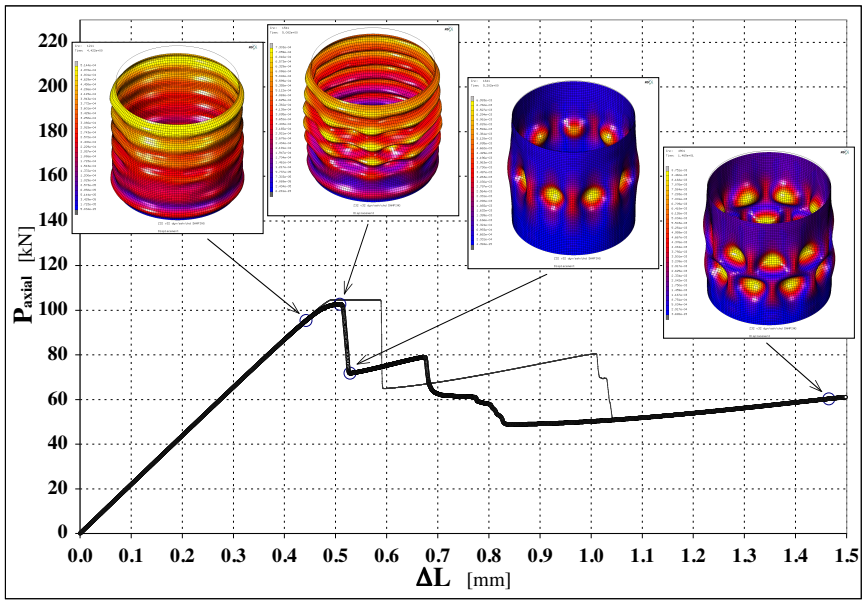

Figure 9. *Dynamic FE analysis results of cylinder Z 32 with measured imperfections*

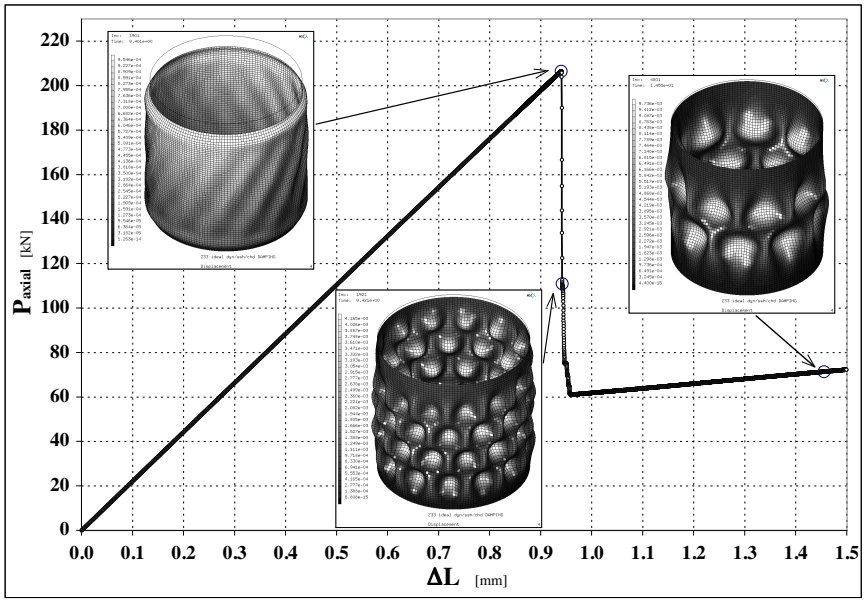

Figure 10. *Dynamic FE analysis results of cylinder Z 33 with ideal geometry*

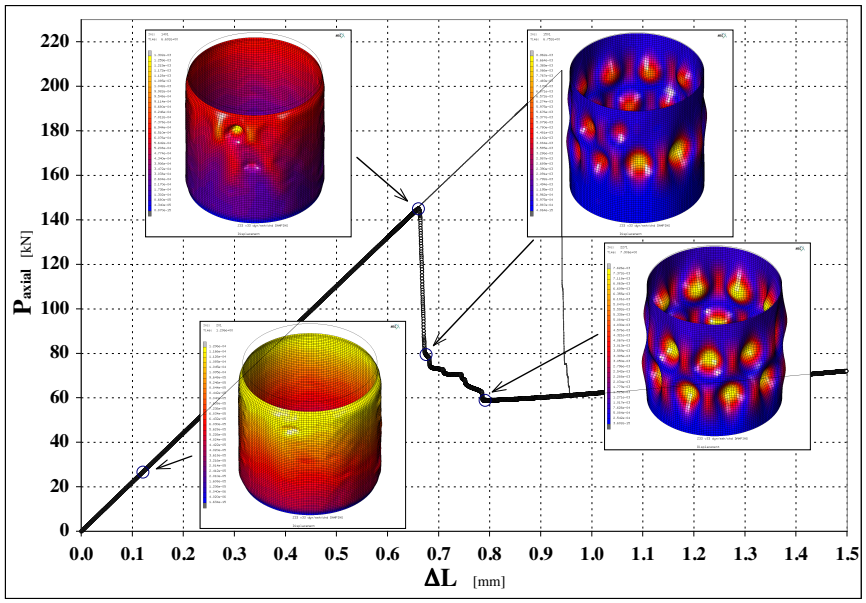

Figure 11. *Dynamic FE analysis results of cylinder Z 32 with measured imperfections*

6. Alternative analysis input parameters

The above-mentioned considerations concerning damping and compression velocities in dynamic FE analysis are also valid for laminated cylinders. The presented results were obtained by the use of MSC.MARC 2000 with its newer "Single Step Houbolt" operator for time integration implemented [CHU 94]. This implicit operator

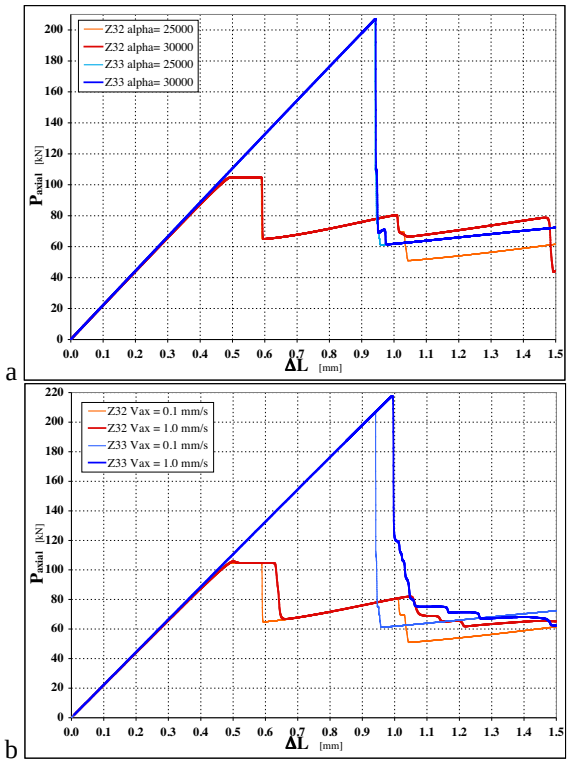

Figure 12. *Influence of inertia damping (a) and compression velocity (b) to the dynamic FE analysis of cylinder Z 32 and Z 33*

is, in linear case, unconditionally stable. Therefore the number of time steps needed to guarantee equilibrium is significantly smaller than needed using an explicit operator which is only stable for time steps smaller than the shortest natural oscillation period of the FE model [BAT 90]. The needed number of time steps in the presented cases with the mentioned input parameters and real densities are in the range of 5000, whereas comparative tests using ABAQUS/Explicit needed about 10 million time steps. Since the –per step– faster matrix system handling of the explicit operator was not able to reduce the analysis duration to the range of the implicit operator, the use of explicit operators can not be recommended as long as the structure is not an object of a crash analysis. Crash analyses deal with significantly higher deformation velocities and shorter process durations, and therefore the required number of stable time steps

is considerably smaller. In Figure 12 the influence of different parameters on the dynamic FE analysis of cylinder Z 32 and Z 33 is shown. To what extent such parameters can be modified by the user depends on the available FE program.

Useful damping parameters are difficult to estimate. The presented values were finally found by "trial-and-error", dealing with the collapse of cylinder Z 33 with ideal geometry. Fig. 12a shows the effects of increasing the damping parameter α (pure inertia dumping) from 25 000 to 30 000. Cylinder Z 33 is almost not affected, but for cylinder Z 32 the change from the 1st to the 2nd post-buckling state has to be expected at a smaller value of axial shortening.

The chosen compression velocity of 0.1 mm/s leads to almost identical buckling loads than those achieved by nonlinear static analysis. Possible over-shoots and additional axial forces through damping are small and may be neglected. Fig. 12b manifests the change of the velocity to 1 mm/s: over-shoots are then noticeable for both specimens.

The shell element masses may be distributed throughout their volume or concentrated in points (e.g. element centre). Using an explicit operator the mass matrix should be diagonal, therefore lumped mass is standard in this case. Comparative calculations yielded the discovery that the sensitivity of this parameter may be neglected for both specimens.

7. Conclusions

For the purpose of calibrating some dynamic transient FE analyses of a thin-walled isotropic circular cylinder were performed. Compared with available high-speed movies the results show good agreement in the buckling behaviour of such cylinders. Thereafter, missing comparable recordings, dynamic FE analyses of two CFRP cylinders, differing only in the opposing sign of their coupling stiffness, were conducted to investigate the noticeable differences between their static buckling and stable post-buckling patterns. The analyses yielded very similar results to nonlinear static FE analyses for the buckling loads. By introducing measured imperfections as initial geometry important findings from previous studies on the imperfection sensitivity of such carbon cylinders could also be demonstrated: (i) laminated cylinders with maximised buckling resistance tend to be imperfection sensitive in buckling analyses, and (ii) considering imperfections in FE analyses nonlinear procedures are mandatory.

Numerical buckling test simulations are possible but time consuming. Presented dynamic transient FE analysis assumes rather low compression velocities. Thus, to guarantee stepwise equilibrium damping has to be introduced. The choice of adequate damping parameters is the most demanding part, as the calculation time has to be kept to reasonable limits. Nevertheless, presuming that the boost of the CPU rates proceeds as hitherto, in the not so distant future the dynamic transient FE analysis method might become a widely-used tool for buckling analyses – as a complement to static analyses.

8. References

[BAT 90] BATHE K.-J., *Finite-Elemente-Methoden*, Springer, Berlin and Heidelberg, 1990.

[BIS 00] BISAGNI C., "Numerical analysis and experimental correlation of composite shell buckling and post-buckling", *Composites: part B*, vol. 31, 2000, p. 655 – 667.

[CHU 94] CHUNG J., HULBERT G. M., "A familiy of single-step Houbolt time integration algorithms for structural dynamics", *Comput. Methods Appl. Mech. Engrg.*, vol. 118, 1994, p. 1 – 11.

[ESS] ESSLINGER M., MEYER-PIENING H.-R., "Beulen und Nachbeulen dünnwandiger Schalen - Isotroper Kreiszylinder unter Axiallast", Institut für den wissenschaftlichen Film, Göttingen, Germany, B 1050T.

[GEI 02] GEIER B., MEYER-PIENING H.-R., ZIMMERMANN R., "On the influence of laminate stacking on buckling of composite cylindrical shells subjected to axial compression", *Composite Structures*, vol. 55, num. 4, 2002, p. 467 – 474.

[KRO 86] KROEPLIN B., DINKLER D., "Dynamic versus static buckling analysis of thin walled shell structures", HUGHES T. J. R., HINTON E., Eds., *Finite Element Methods for Plate and Shell Structures*, vol. 2, Pineridge Press Ltd., Mumbles, Swansea, UK, 1986.

[MEY 01] MEYER-PIENING H.-R., FARSHAD M., GEIER B., ZIMMERMANN R., "Buckling Loads of CFRP Composite Cylinders under combined axial and torsion loading - experiments and computations", *Composite Structures*, vol. 53, num. 4, 2001, p. 427 – 435.

[WUL 02] WULLSCHLEGER L., MEYER-PIENING H.-R., "Buckling of geometrically imperfect cylindrical shells - definition of a buckling load", *Int. J. of Non-linear Mechanics*, vol. 37, 2002, p. 645 – 657.